International Journal of Control and Automation
Vol. 8, No. 4 (2015), pp. 259-372
http://dx.doi.org/10.14257/ijca.2015.8.4.33

The Development and Implementation of a Low-Cost Integrated Control System for Aerial Survey

Liqing Zhou[12], Yan Zhang[1], Shu An[1], Zhenhao Pan[1] and Ke Wang[1]

[1]*School of Electronic Information, Wuhan University, China*
[2]*Department of Electrical and Computer Engineering, University of Calgary, Canada*
zlq@whu.edu.cn

Abstract

This paper presents the development of a low-cost integrated control system for aerial survey based on pan-tilt and multi-sensor data fusion. The design of aerial vehicle route planning, pan-tilt mechanical structure and attitude estimation are discussed in detail. A route planning file containing flight paths and automatic exposure points is firstly derived by the route plan software to control the whole aerial photography task. As for the most challenging task, accurate attitude estimation, a custom Kalman filtering hardware module based on FPGA is introduced. The introduced module invokes the build-in multipliers of FPGA to achieve Kalman filtering hardware implementation, which leads to a rapid attitude estimation. After that mechanical structure of a specialized pan-tilt is designed and fabricated to adjust the camera attitude to the vertical direction of the ground plane. The practice aerial survey is also conducted to evaluate the accuracy and performance of designed control system. Our studies indicates that with the designed control system, it would be feasible to configure an aerial survey system while cooperate with professional aerial camera or some other civil cameras, which will make it easier to focusing on evaluation of aerial survey concepts and approaches.

Keywords: *aerial survey, aerial vehicle route planning, pan-tilt, Kalman filter, multi-sensor data fusion keyword*

1. Introduction

Aerial survey is a geomatics method of collecting information by using aerial photography, LiDAR or from remote sensing imagery [1]. It has demonstrated a great potential to some extent and widely used in resource exploration, agricultural development, water conservancy projects and other key construction projects.

Currently there are quite a few companies and research laboratories that have addressed or produced such survey systems. Gleitsmann, L. in Goettingen University presented a method for survey flight that could deal with far less than ideal weather conditions was developed and tested [2]. Xiaoguang Zhao et al. development a topographic survey system to acquire initial 3D ground model using active laser range sensor on a low-flying helicopter platform [3]. Cui Hongxia et al. combined four individual digital cameras to achieve high ground coverage and enlarge base-height ratio [4]. Consequently the application is also reported [5-6]. Jiayuan Lin and his team introduced the practical application of unmanned aerial vehicles for mountain hazards survey [7]. Currently most of the researches focus on aerial imaging method, but there are other two core issues in the aerial photography, one is aerial vehicle route planning and the other is the self-stable pan-tilt. Aerial vehicle route planning is used to design optimized flight routes in a specified field which can make the aerial photography more effective. During a flight the aerial vehicle will occur roll, pitch and yaw rotations influenced by the wind, wave and current. So a self-stable control unit is indispensable to

ISSN: 2005-4297 IJCA
Copyright ⓒ 2015 SERSC

the system to adjust the attitude of the camera. Some commercial integrated aerial survey equipment can achieve such control function, however, it is a high-cost platform, particularly if one intends to do some customized improvement. This paper presents a development of a low-cost integrated control system for aerial survey based on pan-tilt and multi-sensor data fusion, which will make it easier for researchers on aerial survey to focus on evaluation of aerial survey concepts and approaches.

This paper is organized as follow. Section 2 addresses the overall design issues and considerations. Section 3 focuses on the software design of aerial vehicle route planning. Section 4 describes the mechanism structure design and implementation of pan-tilt. Section 5 explains the attitude estimation. The experimental results and conclusions are given in Section 6 and 7, respectively.

2. System Design

The system is mainly composed of three parts, namely aerial vehicle route planning, self-stable pan-tilt aerial and attitude estimation. Aerial vehicle route planning is done before the plane taking off. Its primary mission is to derive flight routes and exposure points and then store the information as a route file to a SD card. Self-stable pan-tilt is the core in whole system and it adjusts the attitude of camera.

As shown in Fig 1, the system is established based on a three-degree-of-freedom pan-tilt, it can adjust camera's attitude in roll angle, pitch angle and yaw angle. Small-volume, Light-weight and great bearing capacity has made up our pan-tilt greatest characteristics.

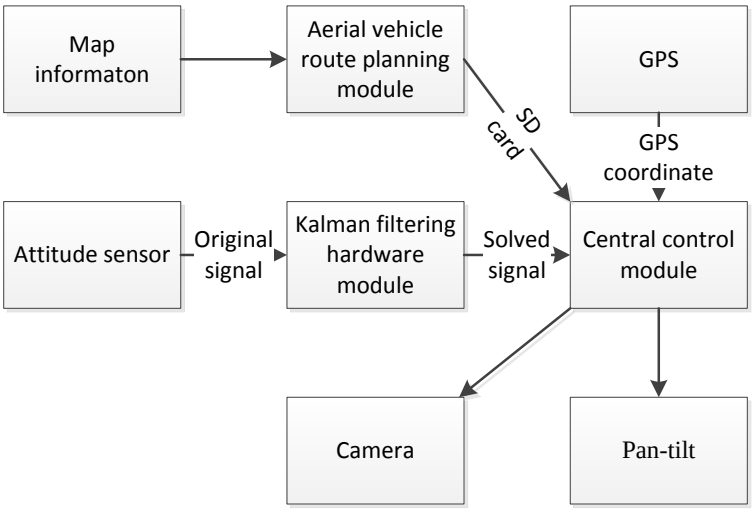

Figure 1. Block Diagram of Control System

Original data measured by attitude sensor contains error under the noise background. In this system, original data is processed in real time by Kalman filter to reduce the error.

Central control module is established by a NIOS software core. What it mainly does is dealing with information about camera attitude and GPS coordinate. It generates corresponding control signal for pan-tilt after getting correct camera attitude. Since it is not complicated when attitude angle changes, we adopt PID algorithm to control pan-tilt, and we use genetic algorithm to set parameters of PID to avoid unnecessary debugging.

Meanwhile, central control module generates interrupt signal to trigger the camera to take a picture when the plane reaches exposure point.

 Copyright ⓒ 2015 SERSC

3. Aerial Vehicle Route Planning

The function of this module is to derive flight routes and exposure points and then store the information as a route file to a SD card for the use of airline guiding and camera control.

The preparation work is to figure out the actual size of area limited by each photo. Set proper value of camera focus, CCD size and flying height to satisfy the accuracy needs. The relation between them is:

$$\frac{Focus}{Height} = \frac{CCD\ Width}{Aera\ Width} = \frac{CCD\ Length}{Aera\ Length} \tag{1}$$

Then, the overlap needs to be set. Generally, the forward overlap is 56%~75%, and the side overlap is 13% ~35% [8].

The area size limited by one photo and the overlap rate between photos are the two key factors in route planning.

3.1. Coordinates of Exposure Points

After loading the boundary data of the map, the software will search the data to find out the maximum and minimum value of latitude (P_a , P_b) and longitude (P_c , P_d).The four values determine a rectangle region which covers the boundary area. The array of exposure points can be worked out based on the forward and side overlap [9]. The staggered photos located on each point cover the whole map area. It is easy to establish the flight route after the array value of exposure points being worked out.

A parameter called boundary factor needs to be considered, it usually takes 50% on the basis of experience.

Then choose the direction along latitude as x-axis to calculate the horizontal coordinate values of exposure points. Assume the overlap rate in vertical direction is O_y , the actual width of area limited by one photo is D and the total amount of values is N_y .

The width of map area needed to cover W_y is:

$$W_y = ((1 - O_y) \cdot (Y_n - 1) + 1) \cdot D \tag{2}$$

The total amount of the horizontal coordinate values N_y is:

$$N_y = (W_t - D) / (1 - O_y) / D + 1 \tag{3}$$

To satisfy the coverage width, get the results in round number and plus one:

$$N_y = [(W_t - D) / (1 - O_y) / D + 1] + 1 \tag{4}$$

The minimum coverage width C_w is:

$$C_w = P_a - P_b + D \tag{5}$$

When $W_y = C_w$, N_y can be calculated.

Besides, the mid latitude value M_l is:

Copyright ⓒ 2015 SERSC

$$M_l = (P_a + P_b) / 2 \tag{6}$$

So the horizontal coordinate array of exposure points Y_j is:

$$Y_j = M_l + (j - N_y / 2 - 1/2) \cdot (1 - O_y) \cdot D \tag{7}$$

Where $0 \le j < N_y$.

In the same way, the result of vertical coordinate array X_i can be got. The point (X_i, Y_j) is just the exposure point which should be figured out.

3.2. Elimination of Needless Points

It is obvious that there are lots of exposure points needless if adopt the method above, those points should be removed.

If choose latitude direction as x-axis, on each Y_j, there is a line connected by different X_i, which can be regarded as one airline. On each line, limit the range between $Y_j - D$ and $Y_j + D$, and then compare the maximum and minimum x-coordinate value of map edge points with the exposure points. Finally remove the extra exposure points whose x-value out of the map.

Since the plane can't turn around instantly to get into another flight route, 2 or 3 points are added to lengthen the airline.

3.3 Flight Route Linking

Final step is to link all the flight routes. Firstly, choose the direction by comparing N_x and N_y. For example, choose latitude direction as x-axis if N_y is smaller. As the first flight route is made up by (X_i, Y_0), assume the minimum X_i on this line is A, and the maximum X_i is B. So the first flight route starts from point (A, Y_0) to point (B, Y_0).

However, assume the maximum X_i in flight route Y_1 is C, and if C is bigger than B. Then the end of flight route should be changed from (B, Y_0) to (C, Y_0).

Following the rules above, flight route linking is finished when the final terminal exposure point is linked.

We tested this module by processing the map data of Wuhan University. The results are shown in Fig 2. As we can see, the black lines are the outline of Wuhan University and the blue lines are the flight paths. All the exposure points are also marked on each path. The figure verifies the correctness of this module.

 Copyright ⓒ 2015 SERSC

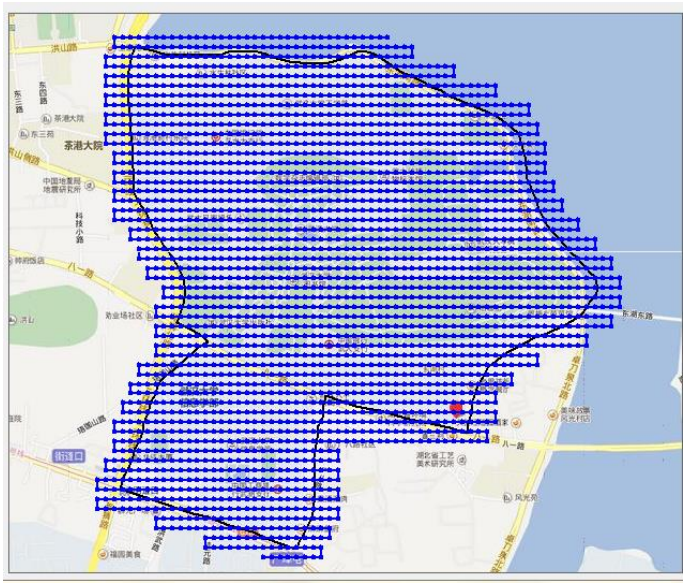

Figure 2. Aerial Vehicle Route Planning

4 Pan-tilt Design

The pan-tilt is applied as a support of installing and fixing cameras. A pan-tilt with three-degree-of-freedom is needed in the system. With the help of pan-tilt, it is easier to adjust the angels in 3 axes to make sure the vertical photography [10].

4.1 Design of Mechanical Structure

As shown in Fig 3, the pan-tilt can be divided into three parts. The outmost layer including motor is fastened to the aircraft while Gear B fixed on the frame of pan-tilt in the second layer. Gear B is driven by gear A meshed with the gear and Gear A is transmitted by a synchronous motor controlled by a controlling circuit. The second layer is designed similarly. The innermost motor controls Gear C which can drive gear D. The camera is placed in the fixed position of cylinder which is pinned to Gear D.

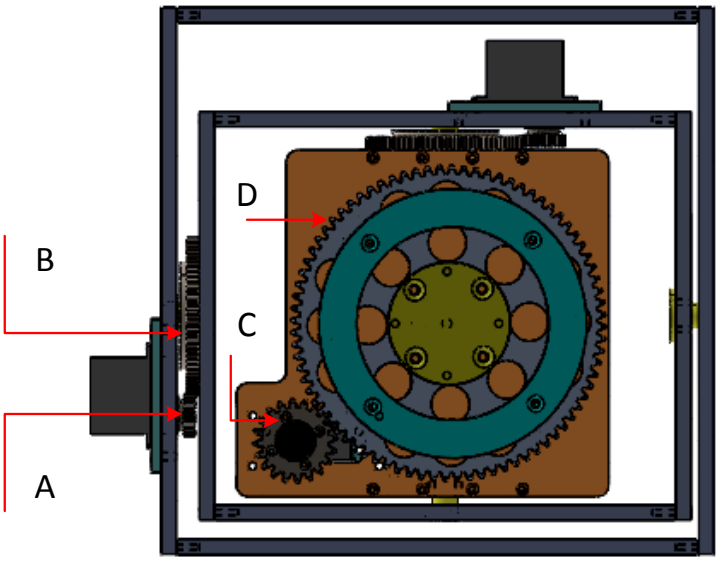

Figure 3. Mechanical Structure of Pan-tilt

Copyright ⓒ 2015 SERSC

There are two details need more attention during the design procedure. On the one hand, the big gear of the innermost must be fixed while its movement must be independent. On the other hand, the sight of camera may be blocked by the frames. To solve the first problem perfectly, a step beam with cap and punch from one end are designed. The cap is pinned to the big gear and screw is used to secure the beam. As for the second problem, cylinder which should be fixed on Gear D and out of the main body is used as a platform to hold the camera.

4.2 Selection of Motor

Considering that the three parts are independent and the capacity of the outmost motor is the biggest, the selection of motor is based on the capacity of the outmost part [11].

The total weight excludes the outmost part is 5kg, the friction coefficient is 0.3, the distance between mass and the rotational axis is 50cm. It can be calculated that the motor torque should be larger than 7.5kg·cm. DM47111 steering gear which can rotate turns continuously follows up with the requirement.

4.3 Design of Transmission Mechanism

The transmission mechanism is the key-point of pan-tilt, hence the high precision of gear drive is the guarantee of accurate controlling. With the reference of Precision Machinery Fundamentals, the steps of designing gears are as follows.

1) According to the design requirement and the size of pan-tilt, determine the type and materials of gear, the transmission ratio and the number teeth.

2) Design with the limit of contact fatigue strength and accurate the bending intensity of tooth root. Look up tables to get the parameter in the formula and then use it to calculate the module.

3) Set the minimum diameter of shaft and then calculate the equivalent dynamic load and the service life of deep groove ball bearings.

The material of spur gear is 45# steel modulation with the harness 200HBS. The mechanical structure accomplished the transmission at a 1:4 ratio and the specific sizes are summarized in table 1.

Table 1. The Specific Sizes of Gears

	Diametrical Pitch	Teeth	Teeth thickness	Pitch Diameter
Gear A	1	20	10	20
Gear B	1	80	10	80
Gear C	2	20	10	40
Gear D	2	80	10	160

According to the analysis, the gears fully meet the design requirement. The minimum diameter of shaft is 6mm, the equivalent dynamic load is 50N and the service life is 2.49×10^7h.

5. Accurate Attitude Estimation based on Kalman Filtering Hardware Module

Kalman filtering hardware module is the key part in whole system, the central control module can’t get the correct attitude without processing original data by it.

 Copyright ⓒ 2015 SERSC

Firstly we build a coordinate system like Fig 4. $\theta_x, \theta_y, \theta_z$ stand for yaw angle, roll angle, pitch angle, G_x, G_y, G_z are three axes acceleration from accelerometer data, W_x, W_y, W_z are three axes angular velocity from accelerometer data. Formula (8) shows the relationship between them.

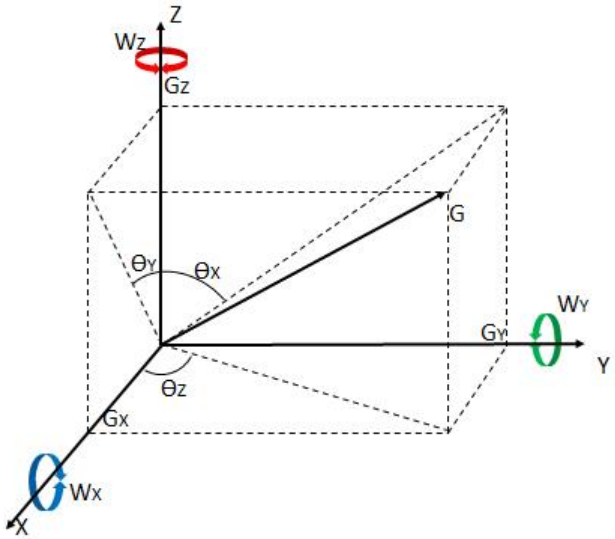

Figure 4. Definition of Coordinate System

$$\begin{cases} \sin\theta_x = G_y / \sqrt{G_y^2 + G_z^2} \\ \sin\theta_y = G_x / \sqrt{G_x^2 + G_z^2} \\ \sin\theta_z = G_y / \sqrt{G_x^2 + G_y^2} \\ \Delta\theta x = W_x \times \Delta T \\ \Delta\theta y = W_y \times \Delta T \\ \Delta\theta z = W_z \times \Delta T \end{cases} \tag{8}$$

Where ΔT is the sample period, $\Delta\theta$ is the angle variation in ΔT time.

5.1 Kalman Filter Model

The Kalman filter, also known as linear quadratic estimation (LQE), is an algorithm that uses a series of measurements observed over time, containing noise and other inaccuracies, and produces estimates of unknown variables that tend to be more precise than those based on a single measurement alone. More formally, the Kalman filter operates recursively on streams of noisy input data to produce a statistically optimal estimate of the underlying system state.

There are two important equations of Kalman Filter as follows:

$$\begin{cases} X_{k+1} = \Phi_{k+1,k} X_k + T_{k+1,k} U_k + \Gamma_{k+1} W_k \\ Z_{k+1} = H_{k+1} X_{k+1} + V_{k+1} \end{cases} \tag{9}$$

Copyright ⓒ 2015 SERSC

Where

$\Phi_{k+1,k}$ is the state transition model; X_k is the previous state; $T_{k+1,k}$ is the control-input model; U_k is the control vector; W_k is the process noise; H_{k+1} is the observation model; V_{k+1} is the observation noise.

To build a Kalman filter model, build a linear model based on gyroscope data firstly [12]:

$$\theta_{k+1} = \theta_k + (U_k - \beta_k)\Delta T \tag{10}$$

Where

θ_k is Attitude angle; U_k is Gyroscope data; β_k is the error of gyroscope data; ΔT is the sample period.

Because there are little variation about the error of gyroscope data, $\beta_{k+1} = \beta_k$. Since W_k has little effect on the system, $W_k = 0$.

Establish the matrix state equation based on the linear model above secondly.

$$\begin{bmatrix} \theta \\ \beta \end{bmatrix}_{k+1} = \begin{bmatrix} 1 & -\Delta T \\ 0 & 1 \end{bmatrix} \begin{bmatrix} \theta \\ \beta \end{bmatrix}_k + \begin{bmatrix} \Delta T \\ 0 \end{bmatrix} U_k \tag{11}$$

Where

$$x = \begin{bmatrix} \theta \\ \beta \end{bmatrix}, \Phi_{k+1,k} = \begin{bmatrix} 1 & -\Delta T \\ 0 & 1 \end{bmatrix}, T_{k+1,k} = \begin{bmatrix} \Delta T \\ 0 \end{bmatrix} \tag{12}$$

Follow the steps following finally.

Step1: Update state prediction based on the gyroscope data U_k:

$$X_{k+1} = \Phi_{k+1,k} \hat{X}_k + T_{k+1,k} U_k \tag{13}$$

Step2: Calculate the observation noise based on the Accelerometer data Z_{k+1}:

$$V_{k+1} = Z_{k+1} - H_{k+1} X_{k+1} \tag{14}$$

Step3: Calculate the covariance of the forecast error:

$$\hat{P}_{k+1} = \Phi_{k+1,k} P_k \Phi_{k+1,k}^T \tag{15}$$

Step4: Calculate optimal Kalman gain:

$$K_{k+1} = P_{k+1/k} H_{k+1}^T (H_{k+1} P_{k+1/k} H_{k+1}^T + R_{k+1})^{-1} \tag{16}$$

Step5: Update state estimate:

$$\hat{X}_{k+1} = X_{k+1} + K_{k+1} V_{k+1} \tag{17}$$

Step6: Update estimate covariance:

 Copyright ⓒ 2015 SERSC

$$P_{k+1} = (I - K_{k+1}H_{k+1})\hat{P}_{k+1} \tag{18}$$

Gyroscope and Accelerometer each has its own advantages on measuring attitude angle, it is necessary to complement their advantages to get reliable attitude angle. The model above takes advantage of Accelerometer data to calculate covariance of measurement noise, and take the covariance into calculation process, which has greatly reduced error from attitude angle.

5.2 Implementation of Kalman Filter

Currently there are two main ways to achieve Kalman filter: (1) PC, PC can meet both requirements about accuracy and real-time performance, but it's heavy and expensive. (2) DSP, DSP is small and light, but its instructions are executed in order, it might not meet the requirement about real-time performance when the system is complicated.

There is another method ——FPGA. The parallel structure of FPGA can solve the problem about accuracy and real-time performance well, and most FPGA nowadays is integrated with soft core, so the work of hardware and software can be done in one FPGA chip, which means the weight and cost can also be greatly reduced [13].

The FPGA chip in the system is EP2C35F672C6 made by Altera, there are 33216 logic units, 483840 memory units, 70 multiplier (9 bits) in the chip. When the Kalman filtering module is established already, Resource consumed is shown in Fig 5.

Figure 5. Resources Kalman Filter Consumes

Total logic elements	14,941 / 33,216 (45 %)
Total combinational functions	13,806 / 33,216 (42 %)
Dedicated logic registers	3,989 / 33,216 (12 %)

Besides resource, speed is also important. Fig 6 shows the speed of Kalman filter module.

Figure 6. Kalman Filter Simulation

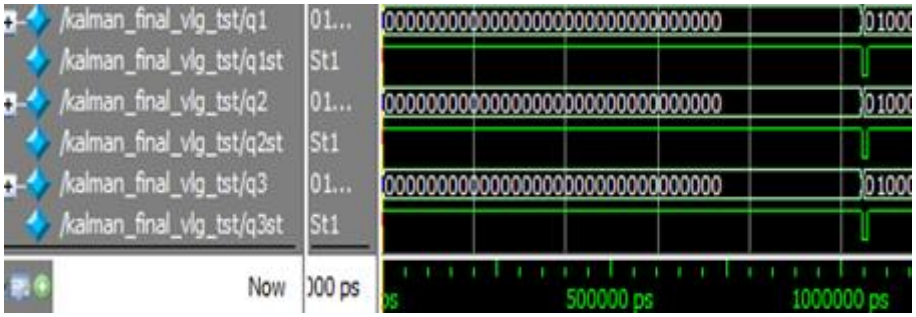

q1, q2, q3 are three attitude angles (roll angle, pitch angle, yaw angle), q1st, q2st, q3st will generate a negative pulse after calculating once. It only takes 1ms to calculate once in Kalman filtering hardware module.

6. Experiments and Practice

To validate the performance of the aerial survey control system, a series of experiments have been conducted.

Copyright ⓒ 2015 SERSC

6.1 Attitude Estimation Performance Test

Experiments were conducted to evaluate the attitude estimation first. The attitude sensor, MPU6050, which combines a 3-axis gyroscope, a 3-axis accelerometer and a digital motion processor in a very small package, outputs 3 angular velocity and 3 acceleration per 20ms. To see the effect from Kalman filter, the raw data of MPU6050 while pan-tilt is shaking is collected by FPGA. Both the raw data and estimation result is shown in Fig 7. Upper half is raw pitch angle data from MPU6050, while bottom half is processed pitch angle via Kalman filter. Comparing these two parts, it is obvious that a clear and accurate attitude will be got after the processing of Kalman filter. The experiment reveals that the attitude estimation hardware module achieved by FPGA can make an accurate estimation from raw data with noise.

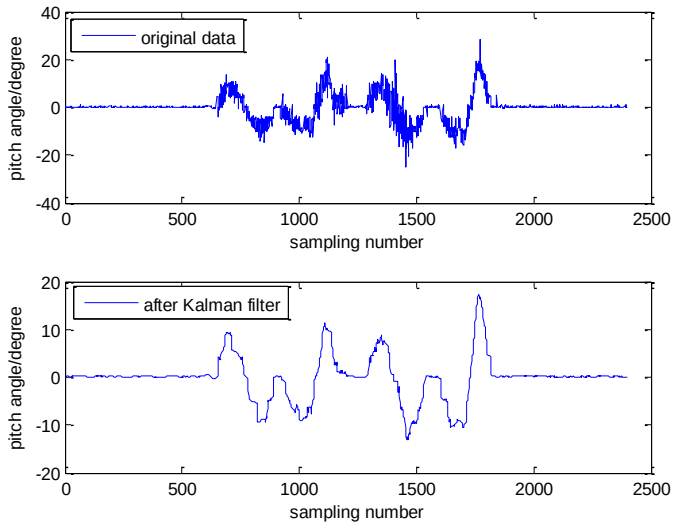

Figure 7. Original Data and Data after Processing

6.2 Practical Application

Until now, tens of flights and photographing tasks are conducted in Hubei, Anhui and Fujian Provinces of China. Fig 8 shows the flying flat and Fig 9 gives the hardware of the control system. The attitude of flying flat is detected by MPU6050 and an accurate estimation is derived by Kalman filter implemented in FPGA. Then the roll, pitch and yaw adjustment parameter calculated by PID algorithm will be sent to the motor driver which will control the pan-tilt rectify the attitude of the camera.

Copyright ⓒ 2015 SERSC

Figure 8. Flying Flat

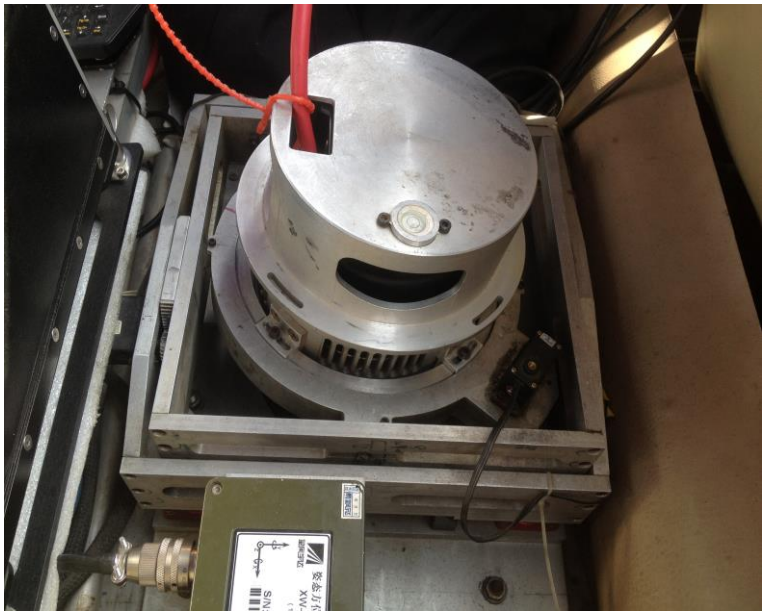

Figure 9. Hardware of Control System

To validate the performance of the entire control system, a comparision between a route adjusted by the designed control system and another route without adjustment was conducted during a practical aerial survey in Nanling, Anhui Province. The aerial vehicle routes are shown in Fig 10 and the aerial images of the two routes are shown in Fig 11. The aerial images of the unadjusted route are obviously rotated because of the wind, while the adjusted route can provide vertical images which can significantly improve the mapping precision and reduce stitching difficulty.

Copyright ⓒ 2015 SERSC

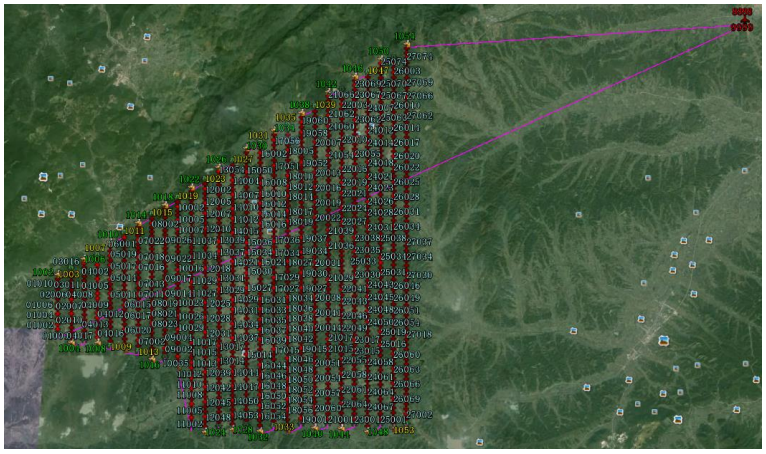

Figure 10. The Aerial Vehicle Routes in Nanling

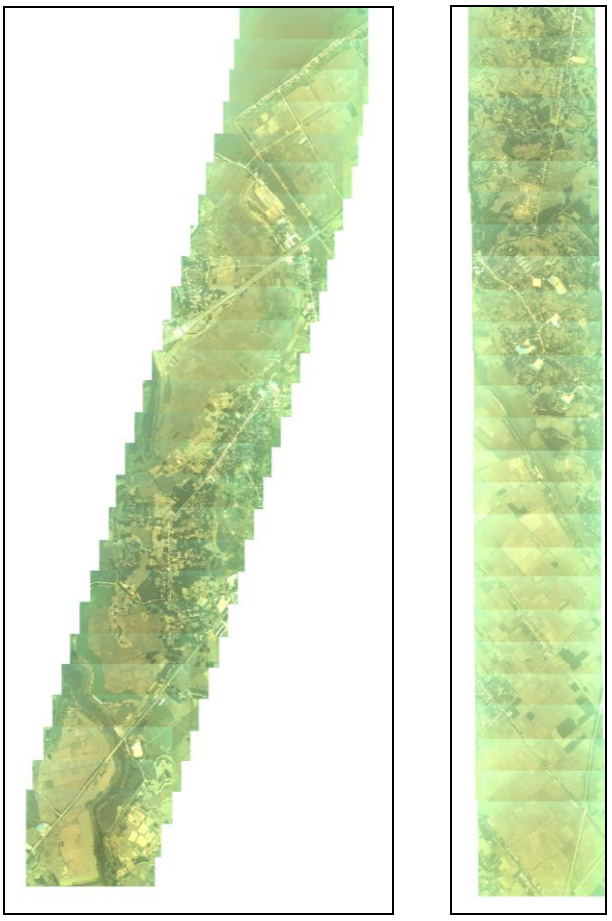

(a) (b)

Figure 11. Aerial Images (a) Unadjusted Route (b) Adjusted Route

7. Conclusions

The development and implementation of a low-cost integrated control system based on pan-tilt and multi-sensor data fusion have been reported. The design of aerial vehicle route planning, pan-tilt mechanical structure and attitude estimation are discussed in detail. The aerial vehicle route planning can make it more effective to conduct aerial

 Copyright ⓒ 2015 SERSC

photography. The accurate attitude estimation and pan-tilt will adjust the camera's attitude to provide vertical images which can significantly improve the mapping precision and reduce stitching difficulty. The practical application based on the development system has demonstrated its usability for aerial survey.

Acknowledgements

This work is supported by National Natural Science Foundation of China (grant No. 61271400, as well as grant No. 61371198). The first author wants to address a special thanks to Doctor Yu Gao of Wuhan Hidi Survey Co. Ltd for his various discussions and advises.

References

[1] C. H. Liu, C. L. Wang and X. L. Liu, "Analysis and application of a close-to-earth digital aero photogrammetry system with over-light plane", Journey of Henan Polytechnic University (Natural Science), vol. 26, no. 5, **(2007)**, pp. 523-528.
[2] L. Gleitsmann and M. Kappas, "Digital multi-image photogrammetry combined with oblique aerial photography enables glacier monitoring survey flights below clouds in Alaska", Geoscience and Remote Sensing Symposium (IGARSS), IEEE International, **(2004)**.
[3] X. G. Zhao, J. Liu and M. Tan, "A Remote Aerial Robot for Topographic Survey", IEEE/RSJ International Conference on Intelligent Robots and Systems, **(2006)**.
[4] H. X. Cui, Z. J. Lin and W. L. Meng, "Virtual Image Generation from Low Altitude Unmanned Aerial Vehicle Digital Aerial Camera", Education Technology and Computer Science (ETCS), First International Workshop, vol. 2, **(2009)**, pp. 697-699.
[5] B. S. Howat and S. Redhead, "The Application & Business Benefits of Aerial Laser Survey Techniques used in the Management of Clearance Infringements", Transmission and Distribution Conference and Exhibition, IEEE PES, **(2006)**.
[6] D. Williams and H. Bisby, "The aerial survey of terrestrial radioactivity", Proceedings of the IEE - Part B: Electronic and Communication Engineering, **(1961)**.
[7] J. Y. Lin, H. P. Tao, Y. C. Wang and H. Zhou, "Practical application of unmanned aerial vehicles for mountain hazards survey", 18th International Conference on Geoinformatics, **(2010)**.
[8] Y. W. Fan, J. Y. Gong, C. G. Tan and R. Y. Wang, "Research on Computer-Assisted DEM-Based Flight Plan of Aerial Photography", First International Conference on Intelligent Networks and Intelligent Systems(ICINIS), **(2008)**.
[9] T. A. Mastor, N. A. Sulaiman, S. Juhari and A. M. Samad. "An Unmanned Aerial Imagery Capturing System (UAiCs): A review of flight mission planning", Signal Processing & its Applications (CSPA), 2014 IEEE 10th International Colloquium, **(2014)**.
[10] J. M. Roberts, P. I. Corke and G. Buskey, "Low-Cost Flight Control System for a Small Autonomous Helicopter", IEEE International Conference on Robotics and Automation (ICRA), **(2003)**.
[11] I. S. Sarwar, "Design, modeling and control of Pan Tilt Platform for unmanned aerial vehicle", M.S. thesis, Dept. Mechatronics Eng., National University of Sciences and Technology, **(2006)**.
[12] B. Erginer and E. Altug, "Modeling and PD Control of a Quadrotor VTOL Vehicle", IEEE Intelligent Vehicles Symposium, **(2007)**.
[13] M. Jew, A. E. Osery and S. Bruder, "Implementation of an FPGA-based aided IMU on a low-cost autonomous outdoor robot", IEEE/ION Position Location and Navigation Symposium (PLANS), **(2010)**.

Copyright ⓒ 2015 SERSC

Copyright ⓒ 2015 SERSC